



HAL
open science

Possible Mechanism for Hole Conductivity in Cu–As–Te Thermoelectric Glasses: A XANES and EXAFS Study

Bhuvanesh Srinivasan, Shuo Cui, Carmelo Prestipino, Alain Gellé, Catherine Boussard-Plédel, Soraya Ababou-Girard, Angela Trapananti, Bruno Bureau, Sergio Di Matteo

► To cite this version:

Bhuvanesh Srinivasan, Shuo Cui, Carmelo Prestipino, Alain Gellé, Catherine Boussard-Plédel, et al. Possible Mechanism for Hole Conductivity in Cu–As–Te Thermoelectric Glasses: A XANES and EXAFS Study. *Journal of Physical Chemistry C*, 2017, 121 (26), pp.14045-14050. 10.1021/acs.jpcc.7b04555 . hal-01613090

HAL Id: hal-01613090

<https://univ-rennes.hal.science/hal-01613090>

Submitted on 11 Oct 2017

HAL is a multi-disciplinary open access archive for the deposit and dissemination of scientific research documents, whether they are published or not. The documents may come from teaching and research institutions in France or abroad, or from public or private research centers.

L'archive ouverte pluridisciplinaire **HAL**, est destinée au dépôt et à la diffusion de documents scientifiques de niveau recherche, publiés ou non, émanant des établissements d'enseignement et de recherche français ou étrangers, des laboratoires publics ou privés.

Possible Mechanism for Hole Conductivity in Cu-As-Te Thermoelectric Glasses: a XANES and EXAFS Study

Bhuvanesh Srinivasan,^[a] Shuo Cui,^[a] Carmelo Prestipino,^[a] Alain Gellé,^[b] Catherine Boussard-Pledel,^[a] Soraya Ababou-Girard,^[b] Angela Trapananti,^[c] Bruno Bureau,^[a] Sergio Di Matteo^{,[b]}*

(a) Institut des Sciences Chimiques de Rennes, UMR CNRS 6226, University of Rennes 1,
35042 Rennes, France

(b) Département Matériaux et Nanosciences, IPR UMR 6251, University of Rennes 1, 35042
Rennes, France

(c) CNR- Istituto Officina dei Materiali (IOM), c/o Department of Physics and Geology,
University of Perugia, 06123 Perugia, Italy

ABSTRACT. Recently synthesized thermoelectric Cu-As-Te glasses have been analyzed by X-ray Absorption Spectroscopy, both near-edge (XANES) and in the extended region (EXAFS), in order to shed light on the mechanism at the basis of the huge increase of conductivity, up to five orders of magnitude, that was found with Cu doping. Experimental data have been modeled by means of multiple-scattering calculations. Our model suggests that the experimental results can be interpreted in terms of a small charge-transfer from Te to Cu, leading to an unexpected positive valence for Te. Interestingly, on the basis of these findings, a global picture explaining the enhancement of electrical conductivity with Cu doping can be proposed: electrical conductivity is determined by the holes created in non-bonding Te 5p orbitals (lone pair) by Cu

acceptors. The critical parameter to increase electrical conductivity is the number of Cu-Te bonds that are formed and not simply the number of Cu atoms.

INTRODUCTION

Thermoelectricity, efficiently converting wasted heat into electricity, can be considered a viable route to solid-state cooling and to power generation. Indeed, recent thermoelectric devices allow for the direct and reversible conversion of thermal and electrical energies^{1,2}, and might soon replace chlorofluoro-carbons as cooling devices. The main paradigm in the present researches on thermoelectric materials is strongly focused on the “phonon glass electron crystal” (PGEC) model²⁻⁴, which proposes an offbeat combination of glass-like low-thermal conductivity and crystal-like high-electrical conductivity. We remind that the final goal for the optimization of a thermoelectric device is to maximize the so-called figure of merit, defined as $ZT = S^2\sigma T/\kappa$, where S is the Seebeck coefficient, σ the electrical conductivity, T the absolute temperature and κ is the thermal conductivity. This explains the search for low- κ and high- σ (and S) materials. In the pursuit of the PGEC model, several frameworks have been analyzed, mostly based on engineering complex crystal structures such as skutterudites or Zintl compounds. In the former case, thermal conductivity is reduced by rattling dopant atoms in cage structure^{5,6}, whereas in the latter a high degree of valence imbalance and disorder is the key to increase the ZT value^{7,8}. Other notable approaches to enhance ZT includes, synergistic nanostructuring^{9,10}; fostering resonant levels by impurities inside the valence band¹¹; quantum confinement of electron charge carriers¹²; and convergence of electronic band valleys^{13,14}. So far the thermoelectric potential was established in several material classes, including tellurides¹⁵⁻¹⁹, selenides^{1,20}, half-heuslers^{21,22} and silicides^{23,24}.

More recently²⁵⁻²⁷, a revival in a different approach to the PGEC principle appeared. It deals with the possibility of designing electrically conductive glassy phases, based on chalcogenide-telluride glasses, which are known to inherently possess high Seebeck coefficient and low thermal conductivity. The main limiting factor in these chalcogenide glasses is their mediocre electrical conductivity. Yet, it was recently found²⁸⁻³¹ that doping glasses with Cu leads to a huge enhancement in the electrical conductivity. For example, the 20% Cu-doping in arsenic telluride shows an increase in σ by almost 5 orders of magnitude (~ 6 S/m)²⁸ compared to the pristine arsenic telluride glass ($\sim 10^{-4}$ S/m), without dismantling the amorphous structure of the glass (i.e., without introducing crystallization) and its characteristic high Seebeck coefficient and low thermal conductivity. In spite of the deep experimental investigation by Lucas *et al.*²⁸, no explanation about the physical mechanism leading to this huge increase in electric conductivity was found. In keeping with the PGEC paradigm, it was advanced³² that a metal-like conductivity takes place even in the glass, due to Cu 4s (or 3d) empty orbitals. Indeed, Cu-atoms were supposed to oxidize with Te, given the relative electronegativity of the two atoms (2.1 for Te and 1.9 for Cu within the Pauling scale). Yet, we believe that this picture needs to be reconsidered in the light of the findings reported in this work. In the following, we present our experimental and theoretical results and then devote the last part of the paper to describe a possible mechanism for the increase of the hole conductivity in the glasses with Cu doping.

METHODS AND RESULTS

The experimental details concerning the synthesis of Cu-As-Te glasses are explained in detail in the Supporting Information (SI). We performed X-ray Absorption Spectroscopic measurements, both near-edge (XANES) and in the extended energy region (EXAFS), at beamline BM23³³ (ESRF, Grenoble), at the K-edge of As, Te and Cu. Measured X-ray

absorption spectra at the As K-edge and at the Te K-edge are shown in Fig. 1. The main result at the As K-edge (Fig. 1(a)) is that Cu doping does not affect significantly the valence of As, as no noticeable chemical shift is present in the As K-edge spectrum with increasing Cu content. The only clear change in the As XANES spectrum is present in the region above 11870 eV, and might therefore be related to structural changes. However, EXAFS data (Fourier transform of the $k^2\chi(k)$ signal, i.e., $|\chi(r)|$ (\AA^{-3})), reported in the inset of Fig. 1(a), show that Cu-doping does not either affect appreciably the local structure around As atoms (in particular, the curves of 2% and 5% Cu-doped compounds are practically identical to that of the undoped compound), so that the changes above 11870 eV should rather be related to further nearest-neighbor shells (e.g. Cu-Te bonds). If we look instead at the Te K-edge, in Fig. 1(b), an appreciable shift of the edge towards higher energy appears with increasing Cu content. We remark that the relative energy shift of Cu_2Te and Te metal with glasses was measured with special care, the former being collected from the transmitted part of the beam measuring the glasses spectra. This implies that Cu atoms mainly affect the environment of Te-atoms and not that of As atoms. EXAFS data at the Te-K edge, not shown, point to the same result, with a clear change with Cu-doping. A quantitative analysis, however, was not possible for the moment, in the absence of a reliable model for the glass structure. We remind that a shift of the main edge towards higher energy is usually interpreted in terms of a positive valence of the absorbing ion. In our case, a positive Te valence, given the absence of changes at the As K-edge, would lead to a negative Cu valence, against a simple application of electronegativity rules.

Because of the counterintuitive result, and as other interpretations might be possible (see Kim *et al.*³⁴ and discussion below), we have decided to analyze it with two different theoretical approaches: *i*) XANES measurements are theoretically interpreted using the FDMNES (Finite

Difference Method Near-Edge Spectroscopy) simulations package³⁵, based on a multiple scattering technique, partitioning the space into muffin-tin spheres close to the atoms and interstitial regions, with projection of the wave function into a spherical-harmonics local basis-set³⁶; *ii*) in parallel, to analyze the Cu-Te charge transfer, we performed ab-initio calculation based on density functional theory. We used projector-augmented-wave (PAW) approach implemented in the Vienna Ab initio Simulation Package (VASP)^{37,38}.

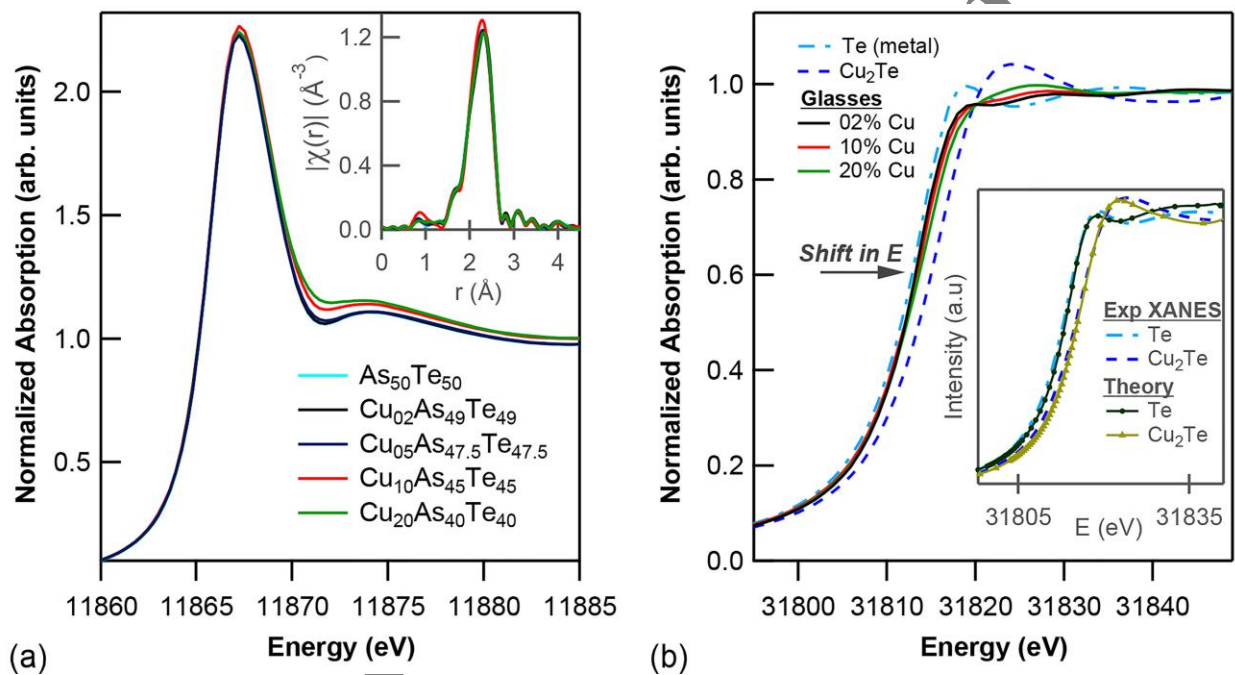


Figure 1. (a) As K-edge XANES spectra of five glasses with increasing Cu content. No noticeable change in the chemical shift appears. Insert shows the Fourier transform of the $k^2\chi(k)$ EXAFS signal which also points to negligible structural changes around As. (b) XANES spectra of three glasses at the Te K-edge, in comparison with Te and Cu_2Te . The chemical shift points to a positive valence of Te ions both in the glasses and in Cu_2Te . The inset shows the very good agreement between FDMNES calculations and experimental spectra.

Though we could not arrive at a definitive conclusion about the local structure of our glasses around Te, yet the close similarity in the XANES spectra of our Cu-As-Te glasses and Cu₂Te, both at the Te K-edge (Fig. 1(b)) and at the Cu K-edge (Fig. 3 below), suggests that their local structure might be close. The glasses and Cu₂Te spectra look very similar also at the Cu-L3 edge (not shown). In particular, from Fig. 1(b), increasing the ratio Cu/Te leads to an increasing positive-energy shift with Cu content, from the glasses up to Cu₂Te. So we decided to study at first the chemical shift of Cu₂Te, described in terms of the Nowotny structure³⁹ (space group *P6/mmm*, N. 191) with Cu-Te distance fixed to 2.56 Å, as obtained from our EXAFS results at the Te K-edge. The inset of Fig. 1(b) shows how well FDMNES ab-initio calculations allow reproducing the relative chemical shift and shapes of Te metal and Cu₂Te spectra. From the analysis of the orbitally-projected DOS of the calculation for Cu₂Te, we get a very slight negative charge on Cu ions (-0.01) and a positive one on Te ions (+0.02). We remark that in the literature a much bigger negative charge on Cu ions (-0.2) was found in Kashida *et al.*⁴⁰, using a self-consistent LMTO approach.

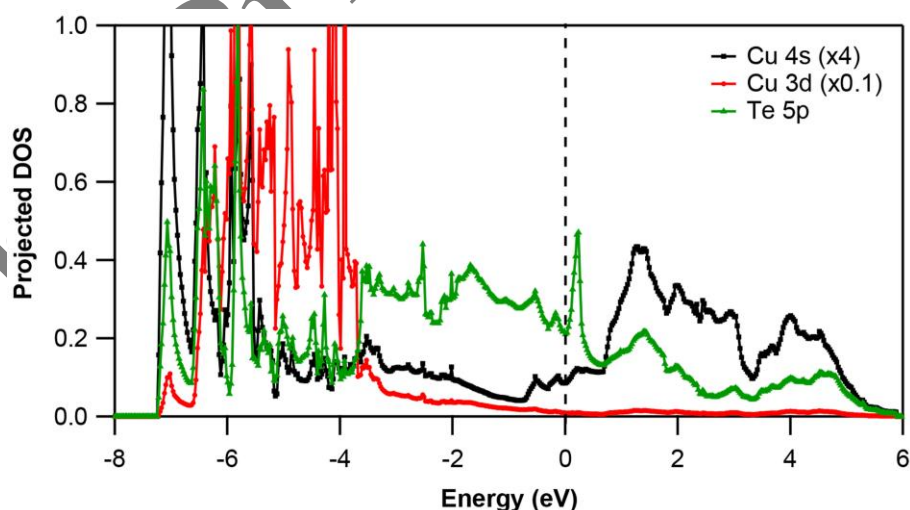


Figure 2. DFT calculations (see text for details): orbitally-projected DOS for Cu₂Te. Cu 3d and 4s energy distribution is compared to Te 5p distribution.

In order to double-check these results within the VASP package we evaluated the charge on each atom following the partitioning of space introduced by Bader^{41,42}. FFT grids were increased up to $24 \times 24 \times 40$. Because of the presence of Cu atoms, the electronic density is expected to be sensitive to the value of the Coulomb repulsion⁴³, that was included (LDA+U) with the approach of Dudarev *et al.*⁴⁴. The calculation was performed with Coulomb repulsion on both 3d states ($U_d = 7.5$ eV) and 5p states ($U_p = 1$ eV). Brillouin-zone integration was performed using a $9 \times 9 \times 5$ Monkhorst-Pack k-mesh, and DOS calculation using a $21 \times 21 \times 13$ mesh. Our results provided a tiny positive value for Cu (+0.008). We should notice that, given the low value of the charge transfer, both our FDMNES and VASP results, differently of the one of Kashida *et al.*⁴⁰, are compatible with the absence of any charge-transfer in Cu_2Te , thereby leading to a purely covalent picture of the Cu-Te bonding with no ionicity. We also remark that, even in VASP calculations, Cu ions can be made slightly negative by increasing the Coulomb repulsion U_p to 2 eV. We remind that the specific value of the Coulomb repulsion can be sample-dependent, because of different screening effects. Usual values for U_p range from 1 to 2 eV and for U_d from 5 to 9 eV. The reason why increasing the Coulomb repulsion of 5p states leads to positive Te ions can be very simply understood from the analysis of the orbitally-projected DOS shown in Fig. 2. The Cu 3d states lay -3.5 to -6.5 eV below the Fermi level and are coupled with 5p bonding levels of Te roughly at the same energy. Non-bonding Te 5p states (the dangling bond), are located from -3.5 eV to zero, in good agreement with XPS/XES measurements⁴⁵, that show Cu 3d levels around -3.5 eV and 5p Te states between -3.5 and zero. In such a situation, the Coulomb repulsion acts in such a way as to rise the energy of Te 5p non-bonding (and empty antibonding) states, compared to Cu states. Given the presence of empty Cu 4s states just above the Fermi energy, this mechanism can lead to some charge transfer from Te 5p to Cu 4s states, thereby making Te slightly positive, in keeping with the finding of Kashida *et al.*⁴⁰. This might

be also what happens in the glasses, as detailed in the following section. We finally remark that this behavior is peculiar to Cu-Te compounds. In fact, though the shift towards higher energy at the Te K-edge compared to Te metal takes place also in CdTe³⁴, the above interpretation cannot be extended to that case because Cd 5s states are totally filled for the isolated atom and the electron charge transfer from Te to Cd cannot take place even if Te 5p levels are raised in energy by the same Coulomb mechanism⁴³. The interpretation given by Kim *et al.*³⁴ for CdTe was rather based on a purely ionic approach with Te⁻² ions, leading to the complete filling of 5p states and to the transition to 6p states, higher in energy. However, this picture is untenable to explain the shift to higher energy of our glasses: even in the hypothesis of a charge transfer from Cu to Te, making Te negative, 2% to 20% Cu-doping would allow only a limited filling of the 5p band, not a complete filling, against the interpretation of Kim *et al.*³⁴.

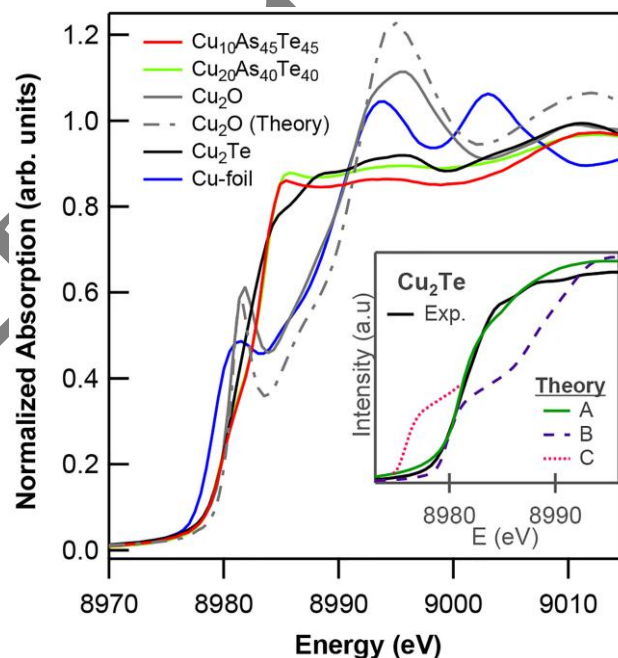


Figure 3. XANES spectra at the Cu K-edge for Cu-doped glasses. The spectra of Cu-metal, Cu₂Te and Cu₂O are shown for comparison of the chemical shift. The FDMNES calculation for

Cu₂O is also shown. Insert shows Cu₂Te raising edge of experimental spectra in comparison with theoretical spectra. Curves A, B and C are explained in the main text.

Before moving back to the glasses, we decided to analyze the chemical shift of Cu₂Te also at the Cu K-edge. Looking at Fig. 3, around 8980 eV, Cu₂Te and the glasses appear to have the same chemical shift as Cu₂O (which is known to be Cu⁺¹), as all edges move to higher energy compared to Cu-metal, Cu⁰. Because of this analogy with Cu₂O, in previous photoemission studies on Cu₂Te⁴⁵, Cu had been attributed the positive valence +1, in apparent contradiction with what stated above. However, the two cases are profoundly different for two main reasons. The first is that O 2p states are much lower in energy than Cu 3d, the latter lying between 0 and -3 eV, the former between -4 eV and -7 eV⁴⁶, so that the pd-Coulomb repulsion does not raise in energy the O 2p, but the Cu 3d. The second is that Cu 3d states are partly empty, with the formation of hybridized 4s-3d_{z²} orbitals leading to incomplete 3d_{z²} shell and occupied Cu 4s states (the so-called Orgel model⁴⁷ of Cu₂O). Therefore its density of states is different than that of Cu₂Te shown in Fig. 2. This difference is confirmed by our FDMNES calculation. For Cu₂Te we used the same input used to describe the Te K-edge (in the inset of Fig. 1(b)), with slightly negative Cu valence and totally filled 3d states. It is shown as curve A in the inset of Fig. 3 and it reproduces correctly the chemical shift of the experimental profile. For Cu₂O the experimental data are quite well reproduced by a FDMNES input with incompletely filled 3d shell (see main panel of Fig. 3). The chemical shift, in particular, is very well described in both cases. In order to understand why the two different chemical valences for Cu₂O and Cu₂Te can lead to the same chemical shift at the Cu K-edge, we performed an analogous FDMNES calculation with the same electronic configuration for Cu as in Cu₂O (i.e., unfilled 3d shell). It leads to a very poor agreement with the experiment (curve B in the inset of Fig. 3), though the chemical shift is the

same. The reason for the failure of the chemical-shift rule at the Cu K-edge for Cu_2Te can be understood reminding that Cu K-edge XANES probes empty 4p states of Cu. In the case of Cu_2Te all Cu orbitals (3d, 4s and also 4p) are slightly lower-lying than the corresponding orbitals in Cu_2O and 5p Te states are much higher in energy than 2p O states. This leads to a band-crossing of the lowest-lying Cu 4p states with the highest-lying Te 5p states and we found with FDMNES that a small amount of Cu 4p states is filled. Extended 4p states are more difficult to handle with VASP calculations and, as they scarcely contribute to the DOS, they have been neglected in Figure 3. If these states had been empty, they would have appeared as a prolongation of curve A, corresponding to curve C in the inset of Fig. 3. Had they been empty, they would have restored the expected negative energy-shift of the Cu_2Te edge compared to Cu_2O and Cu. In this sense, the failure of the chemical-shift rule in this case can be explained as a consequence of accidental band-crossing.

DISCUSSION

A model for glass conductivity - XANES data show that glasses have a chemical shift of the same sign as the Cu_2Te sample. We can therefore extend the interpretation of electron charge transfer from Te to Cu for the glasses as well. Actually, further VASP calculations with less symmetric (monoclinic) local structure of Cu_2Te taken from the literature⁴⁸ show that lower local symmetries can increase the negative charge on Cu compared to the Nowotny structure (still of the order ~ 0.01). Of course, a typical framework valid for crystal calculations might not be simply transferred to glasses, where the dopant is not forced on a lattice site. It is well-known instead that, as exemplified by the famous 8-N rule⁴⁹, the glassy structure usually adapts itself to the dopant coordination, without requiring the generation of valence defects. Yet, if we consider the band scheme derived before for the crystal as a valid input to describe also Cu-As-Te glasses,

this allows not only to explain the XANES data at the As, Te and Cu K-edges for the glasses, but can also fulfill the 8-N rule and lead to a mechanism that explains the increase in electrical conductivity with Cu doping. The latter point is a consequence of the formation of hole doping in the 5p non-bonding states of Te. The mechanism is depicted in Fig. 4b and works in the presence of Cu-Te bonds, which should be therefore maximized in order to optimize the value of σ . The 4s electronic states of copper, just below the energy level of the highest Te 5p non-bonding states (the lone pair), efficiently collect Te 5p electrons and create a hole charge-reservoir in Te 5p energy levels.

We remind that the original framework to describe p-type conductivity in intrinsic amorphous As-Te glasses is the so-called Valence Alternation Pair (VAP) mechanism^{50,51}. In this model, non-bonding states of Te (the lone pair) are unstable with respect to excitations leading to the formation of charged defects states (e.g., a C_3^+/C_3^- center as in Fig. 4a) by thermal electron transitions (in, e.g., $As_{50}Te_{50}$ enhanced by the possibility of forming triple bonds with As atoms). The VAP mechanism of electrical conduction is extremely slow, being determined by both the thermal excitation of non-bonding electrons to antibonding states and by the correlation of two such electron excitations in nearby Te-atoms, so as to form a charge separation (depicted in Fig. 4a). Instead, as shown in Fig. 4(b), the hole formation in the valence band of Te is enormously enhanced by the presence of Cu atoms with empty 4s states just below the higher-lying 5p Te states of the lone pair. In this case, the hole-creating process is much faster, as the lone pair is unstable with respect to the filling of the Cu empty level. We remark that the number of holes created in the valence band of Te by this mechanism does not correspond to the number of Cu atoms, but rather, because of the 8-N rule, to the number of Cu-Te bonds. This simple picture is coherent with the behavior of σ , that increases with increasing Te and decreasing As for fixed

amount of Cu²⁸. This picture calls for the need to find a protocol to optimize the sample preparation so as to minimize the number of Cu-Cu bonds and optimize the number of Cu-Te bonds, for a given amount of Cu-doping.

At fixed hole concentration, the other critical parameter to increase the electric conductivity is the hole mobility, that in our model strongly depends on both Cu-Te and Te-Te bond connectivity. Indeed, once the holes have been formed (with a concentration proportional to the number of Cu-Te bonds), they must be able to hop and, for that, Te-Te bonds are needed. Therefore, the correlation of Cu-Te and Te-Te bond distributions plays a fundamental role in the mobility. This picture can explain why thermal treatments, that modify the global Cu-Te and Te-Te connectivity, affect the value of σ , as found by Lucas *et al.*²⁸, where samples with the same amount of Cu and Te content differ in the value of σ because of different annealing procedures. Interestingly, in this model, the creation of copper islands in the glass would decrease σ because it would not allow the creation of hole-centers. For all these reasons, the Cu-As-Te ternary glasses behave like extrinsic semiconductors with quite high hole concentrations and relatively low hole mobility. If this picture is correct, the logarithmic decrease of resistivity with increasing temperature⁵² should be attributed to an increase of the hole mobility with temperature, rather than a change in the hole concentration.

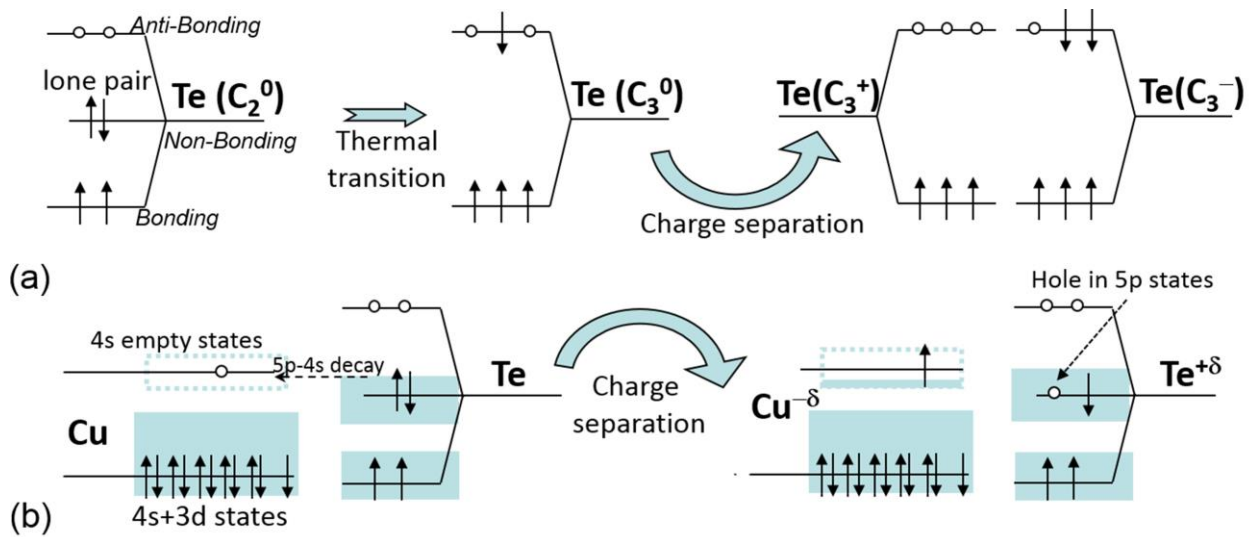


Figure 4. (a) the VAP mechanism of conductivity in undoped chalcogenides: thermal excitation of the lone pair⁵⁰ leads to C_3 neutral defects. Two such neighbor defects can induce charge separation (C_3^+ and C_3^-). (b) Empty Cu-4s levels, with a low-energy tail below the higher-energy level of 5p Te lone pairs, more efficiently increase the hole concentration in the 5p Te orbitals.

To conclude, our XANES measurements at the Te K-edges for Cu-As-Te glasses point to a positive valence for Te, increasing with increasing Cu content (Fig. 1(b)). This is confirmed by multiple-scattering calculation. It is not confirmed by DFT calculations, though the latter do not allow for a definite conclusion on this point. Combining all the experimental findings at As, Te and Cu K-edges with their theoretical interpretation through multiple-scattering and DFT calculations, we find that a small electron charge transfer from Te 5p non-bonding states to Cu 4s empty states is a possible interpretation. These findings suggest an interesting interpretation to explain the huge increase in σ with Cu in these Cu-As-Te p-type glasses. The electrical conductivity is not determined by Cu orbitals but by the holes created in non-bonding Te 5p orbitals. The role of Cu atoms is to act as acceptors, tuning the hole concentration in Te 5p orbitals. The hole conductivity is confirmed by the positive measured Seebeck coefficient in

these doped glasses²⁸⁻³⁰. This picture can be understood as a modification of the VAP mechanism, usually invoked to explain conductivity in chalcogenide glasses^{50,51}. Such a mechanism reckons heavily on the Cu-Te and Te-Te bond connectivity rather than Cu-Cu bonding. These results can lead to more precise investigations of the local environment of these glasses so as to optimize the doping strategies, in order to enhance the thermoelectric performance. Future theoretical and experimental investigations might confirm our prediction: in particular, it would be interesting to look for positive correlations between the increase in electrical conductivity and the increase in Cu-Te bonds by the study of Cu-Te pair distribution function.

ASSOCIATED CONTENT

Supporting Information

Supplementary information: Synthesis of glasses, XANES measurements and FDMNES calculations.

AUTHOR INFORMATION

Corresponding Author

Email: sergio.dimatteo@univ-rennes1.fr; Tel: +33 (0)2 23 23 69 60

Author Contributions

The manuscript was written through contributions of all authors. All authors have given approval to the final version of the manuscript.

ACKNOWLEDGMENT

The authors would like to thank the funding for the project from European Commission's Horizon 2020 research and innovation programs under Marie Skłodowska-Curie ITN actions - CoACH (GA. 642557) and GlaCERCo (GA. 264526). They also acknowledge the European Synchrotron Radiation Facility for providing beamtime and thank Olivier Mathon for assistance during the experiment on beamline BM23.

REFERENCES

- (1) Zhao, L.-D.; Lo, S.-H.; Zhang, Y.; Sun, H.; Tan, G.; Uher, C.; Wolverton, C.; Dravid, V. P.; Kanatzidis, M. G. Ultralow Thermal Conductivity and High Thermoelectric Figure of Merit in SnSe Crystals. *Nature* **2014**, *508*, 373–377.
- (2) Snyder, G. J.; Toberer, E. S. Complex Thermoelectric Materials. *Nat. Mater.* **2008**, *7*, 105–114.
- (3) Terry, T. T. Thermoelectric Materials, Phenomena, and Applications: A Bird's Eye View. *MRS Bull.* **2006**, *31*.
- (4) Takabatake, T.; Suekuni, K.; Nakayama, T.; Kaneshita, E. Phonon-Glass Electron-Crystal Thermoelectric Clathrates: Experiments and Theory. *Rev. Mod. Phys.* **2014**, *86*, 669–716.
- (5) Zhao, W.; Wei, P.; Zhang, Q.; Dong, C.; Liu, L.; Tang, X. Enhanced Thermoelectric Performance in Barium and Indium Double-Filled Skutterudite Bulk Materials via Orbital Hybridization Induced by Indium Filler. *J. Am. Chem. Soc.* **2009**, *131*, 3713–3720.
- (6) Wu, L.; Meng, Q.; Jooss, C.; Zheng, J.-C.; Inada, H.; Su, D.; Li, Q.; Zhu, Y. Origin of Phonon Glass–Electron Crystal Behavior in Thermoelectric Layered Cobaltate. *Adv. Funct. Mater.* **2013**, *23*, 5728–5736.
- (7) Snyder, G. J.; Christensen, M.; Nishibori, E.; Caillat, T.; Iversen, B. B. Disordered Zinc in Zn₄Sb₃ with Phonon-Glass and Electron-Crystal Thermoelectric Properties. *Nat. Mater.* **2004**, *3*, 458–463.
- (8) Toberer, E. S.; May, A. F.; Snyder, G. J. Zintl Chemistry for Designing High Efficiency Thermoelectric Materials. *Chem. Mater.* **2010**, *22*, 624–634.
- (9) Sootsman, J. R.; Kong, H.; Uher, C.; D'Angelo, J. J.; Wu, C.-I.; Hogan, T. P.; Caillat, T.; Kanatzidis, M. G. Large Enhancements in the Thermoelectric Power Factor of Bulk PbTe at High Temperature by Synergistic Nanostructuring. *Angew. Chem. Int. Ed.* **2008**, *47*, 8618–8622.
- (10) Biswas, K.; He, J.; Blum, I. D.; Wu, C.-I.; Hogan, T. P.; Seidman, D. N.; Dravid, V. P.; Kanatzidis, M. G. High-Performance Bulk Thermoelectrics with All-Scale Hierarchical Architectures. *Nature* **2012**, *489*, 414–418.
- (11) Zhang, Q.; Liao, B.; Lan, Y.; Lukas, K.; Liu, W.; Esfarjani, K.; Opeil, C.; Broido, D.; Chen, G.; Ren, Z. High Thermoelectric Performance by Resonant Dopant Indium in Nanostructured SnTe. *Proc. Natl. Acad. Sci. U. S. A.* **2013**, *110*, 13261–13266.
- (12) Hicks, L. D.; Dresselhaus, M. S. Effect of Quantum-Well Structures on the Thermoelectric Figure of Merit. *Phys. Rev. B* **1993**, *47*, 12727–12731.
- (13) Pei, Y.; Shi, X.; LaLonde, A.; Wang, H.; Chen, L.; Snyder, G. J. Convergence of Electronic Bands for High Performance Bulk Thermoelectrics. *Nature* **2011**, *473*, 66–69.

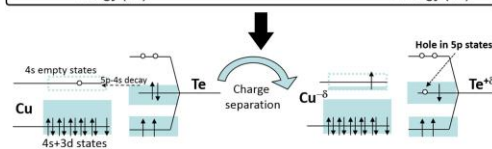
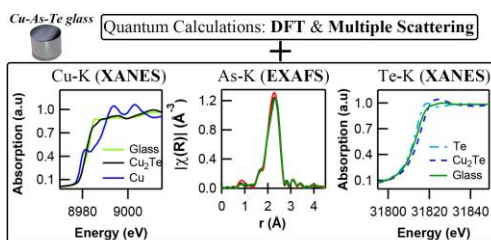
- (14) Banik, A.; Shenoy, U. S.; Anand, S.; Waghmare, U. V.; Biswas, K. Mg Alloying in SnTe Facilitates Valence Band Convergence and Optimizes Thermoelectric Properties. *Chem. Mater.* **2015**, *27*, 581–587.
- (15) Gelbstein, Y.; Davidow, J. Highly Efficient Functional $GexPb_{1-x}Te$ Based Thermoelectric Alloys. *Phys. Chem. Chem. Phys.* **2014**, *16*, 20120–20126.
- (16) Rosenberg, Y.; Gelbstein, Y.; Dariel, M. P. Phase Separation and Thermoelectric Properties of the $Pb_{0.25}Sn_{0.25}Ge_{0.5}Te$ Compound. *J. Alloys Compd.* **2012**, *526*, 31–38.
- (17) Banik, A.; Vishal, B.; Perumal, S.; Datta, R.; Biswas, K. The Origin of Low Thermal Conductivity in $Sn_{1-x}Sb_xTe$: Phonon Scattering via Layered Intergrowth Nanostructures. *Energy Environ. Sci.* **2016**, *9*, 2011–2019.
- (18) Gelbstein, Y. Phase Morphology Effects on the Thermoelectric Properties of $Pb_{0.25}Sn_{0.25}Ge_{0.5}Te$. *Acta Mater.* **2013**, *61*, 1499–1507.
- (19) Hsu, K. F.; Loo, S.; Guo, F.; Chen, W.; Dyck, J. S.; Uher, C.; Hogan, T.; Polychroniadis, E. K.; Kanatzidis, M. G. Cubic $AgPb_mSbTe_{2+m}$: Bulk Thermoelectric Materials with High Figure of Merit. *Science* **2004**, *303*, 818–821.
- (20) Chen, Z.; Ge, B.; Li, W.; Lin, S.; Shen, J.; Chang, Y.; Hanus, R.; Snyder, G. J.; Pei, Y. Vacancy-Induced Dislocations within Grains for High-Performance PbSe Thermoelectrics. *Nat. Commun.* **2017**, *8*, 13828.
- (21) Kirievsky, K.; Shlimovich, M.; Fuks, D.; Gelbstein, Y. An Ab Initio Study of the Thermoelectric Enhancement Potential in Nano-Grained TiNiSn. *Phys. Chem. Chem. Phys.* **2014**, *16*, 20023–20029.
- (22) Zhu, T.; Fu, C.; Xie, H.; Liu, Y.; Zhao, X. High Efficiency Half-Heusler Thermoelectric Materials for Energy Harvesting. *Adv. Energy Mater.* **2015**, *5*, 1500588.
- (23) Gelbstein, Y.; Tunbridge, J.; Dixon, R.; Reece, M. J.; Ning, H.; Gilchrist, R.; Summers, R.; Agote, I.; Lagos, M. A.; Simpson, K.; et al. Physical, Mechanical, and Structural Properties of Highly Efficient Nanostructured N- and P-Silicides for Practical Thermoelectric Applications. *J. Electron. Mater.* **2014**, *43*, 1703–1711.
- (24) Du, B.; Gucci, F.; Porwal, H.; Grasso, S.; Mahajan, A.; Reece, M. J. Flash Spark Plasma Sintering of Magnesium Silicide Stannide with Improved Thermoelectric Properties. *J. Mater. Chem. C* **2017**, *5*, 1514–1521.
- (25) Gonçalves, A. P.; Lopes, E. B.; Rouleau, O.; Godart, C. Conducting Glasses as New Potential Thermoelectric Materials: The Cu–Ge–Te Case. *J. Mater. Chem.* **2010**, *20*, 1516–1521.
- (26) Gonçalves, A. P.; Delaizir, G.; Lopes, E. B.; Ferreira, L. M.; Rouleau, O.; Godart, C. Chalcogenide Glasses as Prospective Thermoelectric Materials. *J. Electron. Mater.* **2011**, *40*, 1015–1017.
- (27) Srinivasan, B.; Boussard-Pledel, C.; Dorcet, V.; Samanta, M.; Biswas, K.; Lefèvre, R.; Gascoin, F.; Cheviré, F.; Tricot, S.; Reece, M.; et al. Thermoelectric Properties of Highly-Crystallized Ge-Te-Se Glasses Doped with Cu/Bi. *Materials* **2017**, *10*, 328.
- (28) Lucas, P.; Conseil, C.; Yang, Z.; Hao, Q.; Cui, S.; Boussard-Pledel, C.; Bureau, B.; Gascoin, F.; Caillaud, C.; Gulbiten, O.; et al. Thermoelectric Bulk Glasses Based on the Cu–As–Te–Se System. *J. Mater. Chem. A* **2013**, *1*, 8917–8925.
- (29) Vaney, J. B.; Delaizir, G.; Alleno, E.; Rouleau, O.; Piarristeguy, A.; Monnier, J.; Godart, C.; Ribes, M.; Escalier, R.; Pradel, A.; et al. A Comprehensive Study of the Crystallization of Cu–As–Te Glasses: Microstructure and Thermoelectric Properties. *J. Mater. Chem. A* **2013**, *1*, 8190–8200.

- (30) Cui, S.; Boussard-plédel, C.; Calvez, L.; Rojas, F.; Chen, K.; Ning, H.; Reece, M. J.; Guizouarn, T.; Bureau, B. Comprehensive Study of Tellurium Based Glass Ceramics for Thermoelectric Application. *Adv. Appl. Ceram.* **2015**, *114*, S42–S47.
- (31) Vaney, J. B.; Piarristeguy, A.; Pradel, A.; Alleno, E.; Lenoir, B.; Candolfi, C.; Dauscher, A.; Gonçalves, A. P.; Lopes, E. B.; Delaizir, G.; et al. Thermal Stability and Thermoelectric Properties of $\text{Cu}_x\text{As}_{40-x}\text{Te}_{60-y}\text{Se}_y$ Semiconducting Glasses. *J. Solid State Chem.* **2013**, *203*, 212–217.
- (32) Yang, Z.; Wilhelm, A. A.; Lucas, P. High-Conductivity Tellurium-Based Infrared Transmitting Glasses and Their Suitability for Bio-Optical Detection. *J. Am. Ceram. Soc.* **2010**, *93*, 1941–1944.
- (33) Mathon, O.; Beteva, A.; Borrel, J.; Bugnazet, D.; Gatla, S.; Hino, R.; Kantor, I.; Mairs, T.; Munoz, M.; Pasternak, S.; et al. The Time-Resolved and Extreme Conditions XAS (TEXAS) Facility at the European Synchrotron Radiation Facility: The General-Purpose EXAFS Bending-Magnet Beamline BM23. *J. Synchrotron Radiat.* **2015**, *22*, 1548–1554.
- (34) Kim, M. G.; Kim, D.-H.; Kim, T.; Park, S.; Kwon, G.; Kim, M. S.; Shin, T. J.; Ahn, H.; Hur, H.-G. Unusual Li-Ion Storage through Anionic Redox Processes of Bacteria-Driven Tellurium Nanorods. *J. Mater. Chem. A* **2015**, *3*, 16978–16987.
- (35) Joly, Y. X-Ray Absorption near-Edge Structure Calculations beyond the Muffin-Tin Approximation. *Phys. Rev. B* **2001**, *63*, 125120.
- (36) Savrasov, S. Y.; Savrasov, D. Y. Full-Potential Linear-Muffin-Tin-Orbital Method for Calculating Total Energies and Forces. *Phys. Rev. B* **1992**, *46*, 12181–12195.
- (37) Kresse, G.; Furthmüller, J. Efficient Iterative Schemes for Ab Initio Total-Energy Calculations Using a Plane-Wave Basis Set. *Phys. Rev. B* **1996**, *54*, 11169–11186.
- (38) Kresse, G.; Joubert, D. From ultrasoft pseudopotentials to the projector augmented-wave method. *Phys. Rev. B* **1999**, *59*, 1758–1775.
- (39) Nowotny, H. Z. Die Kristallstruktur von Cu_2Te . *Metallkunde* **1946**, *37*, 40.
- (40) Kashida, S.; Shimosaka, W.; Mori, M.; Yoshimura, D. Valence Band Photoemission Study of the Copper Chalcogenide Compounds, Cu_2S , Cu_2Se and Cu_2Te . *J. Phys. Chem. Solids* **2003**, *64*, 2357–2363.
- (41) Bader, R. F. W. Atoms in Molecules. In *Encyclopedia of Computational Chemistry*; John Wiley & Sons, Ltd, 2002.
- (42) Tang, W.; Sanville, E.; Henkelman, G. A Grid-Based Bader Analysis Algorithm without Lattice Bias. *J. Phys. Condens. Matter* **2009**, *21*, 084204.
- (43) Wei, S.-H.; Zunger, A. Role of Metal D States in II-VI Semiconductors. *Phys. Rev. B* **1988**, *37*, 8958–8981.
- (44) Dudarev, S. L.; Botton, G. A.; Savrasov, S. Y.; Humphreys, C. J.; Sutton, A. P. Electron-Energy-Loss Spectra and the Structural Stability of Nickel Oxide: An LSDA+U Study. *Phys. Rev. B* **1998**, *57*, 1505–1509.
- (45) Domashevskaya, E. P.; Gorbachev, V. V.; Terekhov, V. A.; Kashkarov, V. M.; Panfilova, E. V.; Shchukarev, A. V. XPS and XES Emission Investigations of D-p Resonance in Some Copper Chalcogenides. *J. Electron Spectrosc. Relat. Phenom.* **2001**, *114–116*, 901–908.
- (46) Wang, Y.; Lany, S.; Ghanbaja, J.; Fagot-Revurat, Y.; Chen, Y. P.; Soldera, F.; Horwat, D.; Mücklich, F.; Pierson, J. F. Electronic Structures of Cu_2O , Cu_4O_3 , and CuO : A Joint Experimental and Theoretical Study. *Phys. Rev. B* **2016**, *94*, 245418.
- (47) Orgel, L. E. Stereochemistry of Metals of the B Sub-Groups. Part I. Ions with Filled D-Electron Shells. *J. Chem. Soc. Resumed* **1958**, 4186–4190.

- (48) Nguyen, M. C.; Choi, J.-H.; Zhao, X.; Wang, C.-Z.; Zhang, Z.; Ho, K.-M. New Layered Structures of Cuprous Chalcogenides as Thin Film Solar Cell Materials: Cu₂Te and Cu₂Se. *Phys. Rev. Lett.* **2013**, *111*, 165502.
- (49) Liu, J. Z.; Taylor, P. C. A General Structural Model for Semiconducting Glasses. *Solid State Commun.* **1989**, *70*, 81–85.
- (50) Kastner, M.; Adler, D.; Fritzsche, H. Valence-Alternation Model for Localized Gap States in Lone-Pair Semiconductors. *Phys. Rev. Lett.* **1976**, *37*, 1504–1507.
- (51) Kolobov, A. V. On the Origin of P-Type Conductivity in Amorphous Chalcogenides. *J. Non-Cryst. Solids* **1996**, *198*, 728–731.
- (52) Gonçalves, A. P.; Lopes, E. B.; Delaizir, G.; Vaney, J. B.; Lenoir, B.; Piarristeguy, A.; Pradel, A.; Monnier, J.; Ochin, P.; Godart, C. Semiconducting Glasses: A New Class of Thermoelectric Materials? *J. Solid State Chem.* **2012**, *193*, 26–30.

Pre-Print Version

TOC GRAPHICS



Pre-Print Version